Magnetic study of *M*-type doped barium ferrite nanocrystalline powders

X. Batlle,[a] M. García del Muro, and J. Tejada
Departament Física Fonamental, Universitat de Barcelona, Diagonal 647, 08028 Barcelona, Catalonia, Spain

H. Pfeiffer, P. Görnert, and E. Sinn
Institut für Physikalische Hochtechnologie, Helmholtzweg 4, 0-6900 Jena, Germany

(Received 8 June 1992; accepted for publication 2 May 1993)

We have studied the static magnetic properties of three different *M*-type doped barium ferrite compounds prepared by the glass crystallization method. The zero-field-cooled (ZFC) and field-cooled (FC) processes have been recorded at low field and they all show the typical features of a small particle system. The ZFC curves display a broad peak at a temperature T_M, which depends on the distribution of particle volumes in the sample. Isothermal magnetization curves $M(H)$ at several temperatures and saturation magnetization M_s as a function of temperature have been measured for the Co-Ti sample ($BaFe_{10.4}Co_{0.8}Ti_{0.8}O_{19}$). The dependence on temperature of the macroscopic magnetic parameters has been analyzed. The distribution of blocking temperatures is studied from the derivative of the remanent-to-saturation magnetization ratio with respect to temperature and it is fitted to a lognormal distribution, leading to a mean blocking temperature $\langle T_B \rangle = (81 \pm 40)$ K. The distribution of volumes of the magnetic unit is also obtained from this fitting. The dependence on temperature of the coercive field follows a T^k-law below 35 K. The value of the k exponent is discussed within the scope of two models: (i) the aligned case ($k=0.5$) and (ii) the random case ($k=0.77$).

I. INTRODUCTION

M-type barium ferrite $BaFe_{12}O_{19}$ has been widely studied because of its applicability in various technological fields, such as microwave devices, permanent magnets, and high-density magnetic and magneto-optic recording media.[1,2] Many efforts have been devoted to the development of a synthesis procedure that leads to a better control of both particle size and morphology, since the conventional ceramic method[3] does not fulfill these aims. Among them (see, for example, Refs. 4–6), the glass crystallization method (GCM)[7–8] appears to be particularly successful in controlling the particle size, from the nanocrystalline regime (mean particle diameter of some tens of angström) to the microscopic region (some microns).

As regard to technological applications, $BaFe_{12}O_{19}$ powders consisting of an assembly of plateletlike single crystalline particles of about 1 μm are suitable materials for permanent magnets. Concerning magnetic recording, the ideal mean particle size is about 0.1 μm. Since the pure compound displays too high a coercive field H_c which precludes its technological applications, $BaFe_{12}O_{19}$ is usually doped with Co^{2+} cations[8–11] which sharply reduce its magnetocrystalline anisotropy.[12] In this framework, the Co^{2+}-Ti^{4+} doping scheme (leading to $BaFe_{12-2x}Co_xTi_xO_{19}$ samples, $0.1 < x \leqslant 1.0$), is the most commonly used,[8–9,11] although other schemes have also been tested, such as the Co-Sn,[10,13] Co-Ti-Sn,[14] and the Co-Ti-Sn-Ge[14] doping schemes. The first was designed in order to reduce the coercive field faster than the Co-Ti substitution, while the other two were studied so as to control the temperature coefficient dH_c/dT. As for the Co-Ti doping, the $x=0.8$ compound seems to be the best one for magnetic recording applications,[8–9,11] since the magnetic structure is still ferrimagnetic, the Curie temperature is well above room temperature and the coercive field is sharply reduced to technologically achievable values. We note that Toshiba has announced the production of a 3.5-in barium ferrite floppy disk with 40 Mb of memory by the spring of 1993 (Ref. 15), which will increase the current memory capacity by about one order of magnitude.

In this paper, we study a particle size region that may lead us to further technological applications, as well as to new fundamental properties: the nanocrystalline region. GCM is proving to be an excellent method to obtain *M*-type doped barium ferrite powders with mean particle size ranging from about 80 to 300 Å (depending on both the thermal treatment and the doping cations), having a plateletlike shape and a narrow size distribution.[8,14] We present the magnetic properties of three different compounds: (i) $BaFe_{10.4}Co_{0.8}Ti_{0.8}O_{19}$ (Co-Ti sample), (ii) $BaFe_{10.3}Co_{0.85}Ti_{0.45}Sn_{0.4}O_{19}$ (Co-Ti-Sn sample), and (iii) $BaFe_{10.4}Co_{0.8}Ti_{0.45}Sn_{0.25}Ge_{0.10}O_{19}$ (Co-Ti-Sn-Ge sample).

II. EXPERIMENT

All samples were prepared by the glass crystallization method. The GCM is characterized by homogenized melt fluxes of Fe_2O_3, BaO, B_2O_3 and of the corresponding oxides of the doping cations (for example, Ti_2O and CoO for the Co-Ti sample) at about 1300 °C, which were amorphized by rapid quenching in a two-roller equipment. Annealing the glass flakes above 550 °C led to the nucleation and growth of the borate and the hexaferrite phases. Barium ferrite particles crystallized to suitable sizes during this treatment and they were isolated by dissolving the

[a]Author to whom all correspondence should be addressed.

 0021-8979/93/74(5)/3333/8/$6.00

matrix in dilute acetic acid in an ultrasonic field. After centrifugation, washing and drying, a fine powder of M-type doped barium ferrite particles with the required stoichiometry was obtained. A more detailed explanation on this procedure is given in Refs. 8 and 14, and references therein.

Magnetization measurements were carried out with an SHE S.Q.U.I.D magnetometer in the temperature range 4.2–300 K and in magnetic fields up to 50 kOe. The zero-field-cooled (ZFC) and field-cooled (FC) processes were recorded at low field (at about 35 Oe) in the same temperature range for the Co-Ti, Co-Ti-Sn, and Co-Ti-Sn-Ge samples, while the isothermal magnetization curves $M(H)$ at some given temperatures and the dependence on temperature of the saturation magnetization were recorded for the Co-Ti compound, in order to compare the experimental results to those reported in the literature concerning bulk powders.

III. RESULTS AND DISCUSSION

We display in Figs. 1(a)–1(c) the ZFC and FC magnetization data for all three compounds studied.

The ZFC curves show a wide maximum at T_M, thus indicating that the magnetic moment of each particle is blocked along its easy magnetization direction at a temperature T_B, which depends on particle volume, anisotropy, and orientation. As the samples are constituted of an assembly of crystallites that present a certain distribution of volumes $f(V)$, each crystallite is blocked at a different temperature T_B, which is not influenced by the easy magnetization direction in absence or in very low magnetic field. Then, we observe experimentally a distribution of blocking temperatures $F(T_B)$ providing a broad peak in the ZFC curve. The maximum of the curves is reached at $T_M \approx 195$, 175, and 245 K for the Co-Ti, Co-Ti-Sn-Ge, and Co-Ti-Sn samples, respectively. T_M is related to the mean blocking temperature $\langle T_B \rangle$ through the distribution of particle volumes (see below). Transmission electron microscopy (TEM) shows that T_M increases with mean particle volume $\langle V \rangle$ ($\langle V \rangle$ is about 1.1×10^5, 0.88×10^5, and 17.5×10^5 Å^3 for the Co-Ti, Co-Ti-Sn-Ge, and Co-Ti-Sn samples, respectively[16]). Besides, the ZFC magnetization (M_{ZFC}) strongly decreases below the peak, since the superparamagnetic-ferromagnetic passage activate the anisotropy which force particle magnetization along the easy axes, which are randomly oriented. The relative decrease of M_{ZFC} is also observed above T_M, as we approach the superparamagnetic region.

There also appears a clear irreversibility between the ZFC and FC measurements. The FC magnetization achieves a nearly constant value below a given temperature T^* (which is always below T_M) and this value is much higher than the ZFC values. The FC magnetization state is nearly an equilibrium state in which below T^* almost all particles have only a positive projection of the magnetization along the magnetic field direction, while the ZFC magnetization state is not a true equilibrium state. If we record the evolution of M_{ZFC} at a given temperature below T_M as a function of time, this value will tend asymptotically to the corresponding FC magnetization value (M_{FC}). The magnetic irreversibility [Fig. 2(a)] is very small for the Co-Ti and Co-Ti-Sn-Ge samples at about room temperature, while it is still high for the Co-Ti-Sn compound, thus indicating that either some degree of magnetic correlation

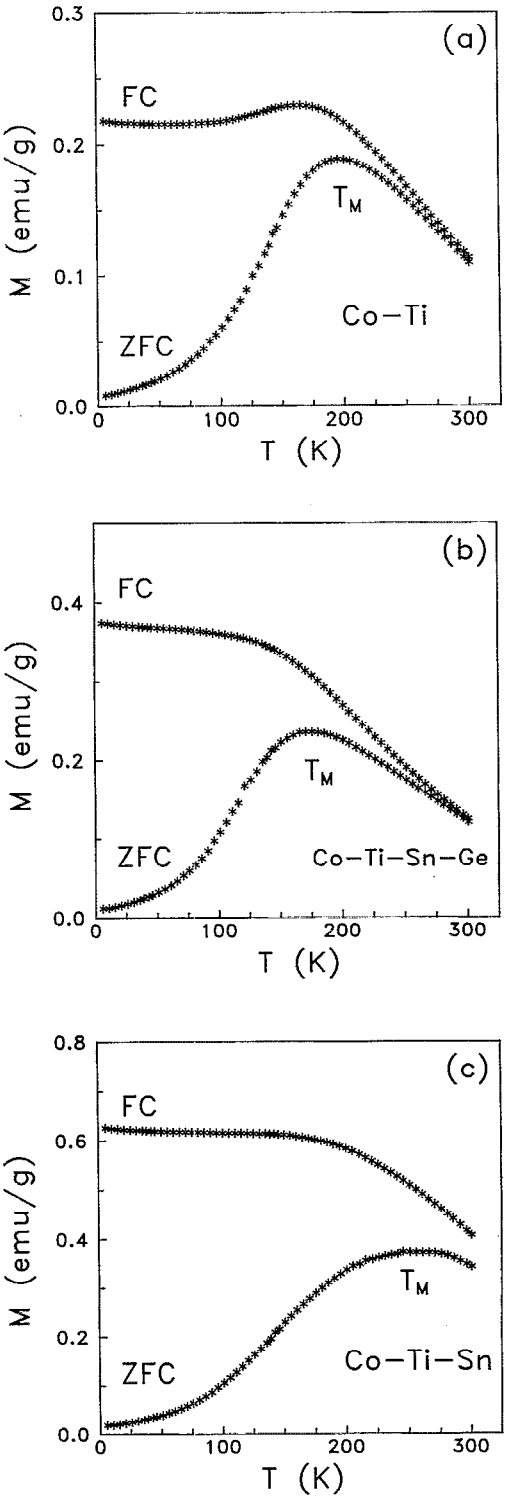

FIG. 1. Zero-field-cooled and field-cooled magnetizations as a function of temperature measured at 35 Oe for (a) the Co-Ti compound, (b) the Co-Ti-Sn-Ge compound and (c) the Co-Ti-Sn compound.

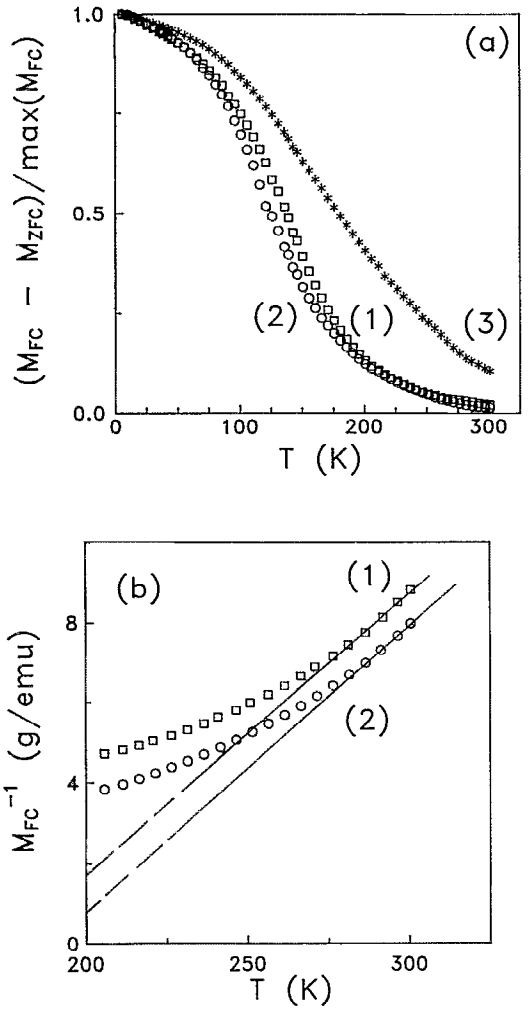

FIG. 2. (a) Difference between the FC and ZFC magnetizations (divided by the maximum FC value) as a function of temperature for (1) the Co-Ti sample, (2) the Co-Ti-Sn-Ge sample, and (3) the Co-Ti-Sn sample. (b) Reciprocal of the FC magnetization as a function of temperature showing the linear regime for (1) the Co-Ti sample and (2) the Co-Ti-Sn-Ge sample.

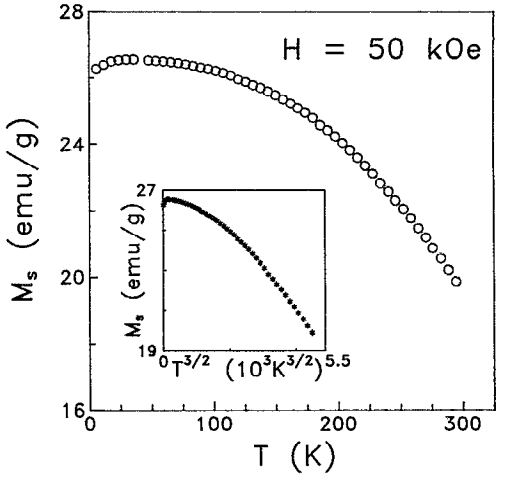

FIG. 3. Saturation magnetization M_s as a function of temperature measured in a magnetic field of 50 kOe for the Co-Ti sample. In the inset, the same data are represented as a function of $T^{3/2}$.

is maintained or there are still a non-negligible amount of blocked particles. In fact, the temperature of the maximum of the ZFC ($T_M \approx 245$ K) is the largest of the three compounds studied.

Therefore, we may obtain a rough estimation of the extrapolated Curie–Weiss temperature ϑ only for the Co-Ti and Co-Ti-Sn-Ge compounds. Although at room temperature most of the particles are already superparamagnetic (see Figs. 1–2 and 6–8), we have to go to higher temperatures in order to accomplish a well-defined linear law M_{FC}^{-1} vs T and a full superparamagnetic regime. We observe in Fig. 2(b) that the linear law is only accomplished between 275 and 300 K, and we find that the extrapolated ordering temperatures ϑ are about 174 and 179 K for the Co-Ti and Co-Ti-Sn-Ge samples, respectively. The positive sign indicates that magnetic interactions among particles are ferromagnetic, and the fitted ϑ values are high. The superparamagnetic regime will extend up to the Curie temperature T_c ($T_c \approx 633$, 621, and 615 K for the Co-Ti, Co-Ti-Sn, and Co-Ti-Sn-Ge samples, respectively).[16]

The dependence on temperature of the saturation magnetization M_s for the Co-Ti sample, measured at 50 kOe, is displayed in Fig. 3. We assume that the decrease of M_s below $T \approx 35$ K is due to the fact that we cannot saturate the sample, since we cannot rotate the magnetic moments of all blocked particles along the magnetic field direction, even at 50 kOe. In the inset of Fig. 3, M_s is shown as a function of $T^{3/2}$, suggesting that the $T^{3/2}$-law[17] does not account for the evolution of M_s. However, the linearity of $\log_{10}[M_s(35\text{ K}) - M_s]$ vs $\log_{10} T$ above 120 K (Fig. 4) with a slope $\alpha \approx 2.7$ [where $M_s(35\text{ K})$ is the saturation magnetization measured at $T = 35$ K and $H = 50$ kOe], might indicate that the observation of the $T^{3/2}$ term is precluded at low temperature due to relaxation effects,

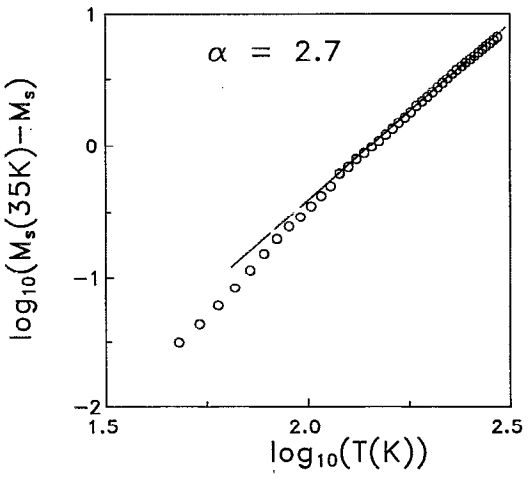

FIG. 4. Log–log plot of $[M_s(35\text{ K}) - M_s]$ as a function of temperature for the Co-Ti sample. The straight line corresponds to the best linear fit of the data, with a slope $\alpha \approx 2.7$.

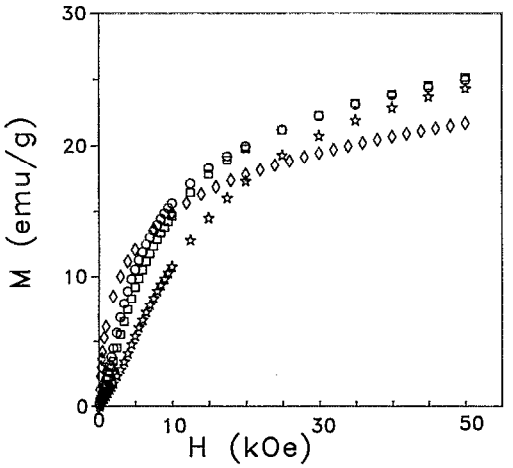

FIG. 5. Isothermal magnetization curves at some temperatures for the Co-Ti sample. [$T=6$ K, (☆); $T=35$ K, (□); $T=50$ K, (○); $T=210$ K, (◇)].

while above ~ 120 K we observe the $T^{5/2}$ term. It should be noted that recent calculations,[18] as well as recent experimental results,[19] for ultrafine particles and clusters (some tens of angström) having fcc and bcc structures have shown that the spin wave picture may also be applied, with an α exponent in the demagnetizing law T^{α} which ranges from 3.0 for the smallest clusters (decreasing almost linearly with the inverse of the cluster diameter) towards the bulk value 1.5.

The isothermal magnetization curves $M(H)$ of the Co-Ti sample have been recorded at several temperatures below the maximum of the ZFC curve T_M. Virgin curves are shown in Fig. 5 and the coercive fields obtained from the hysteresis cycles are displayed in Fig. 6(a). The dependence on temperature of the initial susceptibility χ_{in} (slope of the linear regime M vs H at low fields) is represented in Fig. 7.

Figures 5 and 7 clearly indicate that χ_{in} rapidly increases with temperature, in such a way that, as the zero-field saturation magnetization (the value of the magnetization at zero-field extrapolated from the saturated regime) decreases with temperature, the $M(H)$ curve at a given temperature crosses all $M(H)$ curves corresponding to lower temperatures. This is experimentally observed when $T \geqslant 35$ K (Fig. 5), as expected from Fig. 3 (M_s vs T).

The dependence on temperature of the coercive field H_c is shown in Fig. 6(a). For monodisperse, noninteracting, ferro/ferrimagnetically ordered particles, coercivity is expected to depend on temperature as

$$H_c = H_c(0)(1 - AT^k), \tag{1}$$

where $H_c(0)$ is the coercive field at $T=0$, and A is written as

$$A = [\beta k_B/(K_{\text{eff}}V)]^k, \tag{2}$$

where V is the particle volume and β is a coefficient that depends both on the measuring time of the experiment τ_m

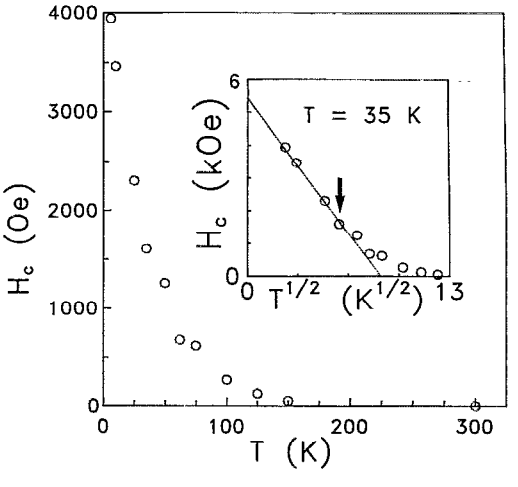

(a)

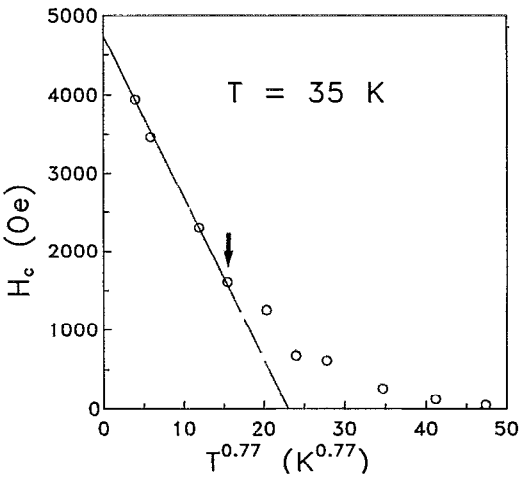

(b)

FIG. 6. (a) Coercive field H_c as a function of temperature for the Co-Ti compound. Inset: H_c plotted as a function of $T^{1/2}$ ($k=1/2$, aligned case). The straight line represents the temperature range where the $T^{1/2}$-law is accomplished. (b) H_c plotted as a function of $T^{0.77}$ ($k=0.77$, random case). The straight line represents the temperature range where the $T^{0.77}$-law is accomplished.

and on the prefactor τ_0 that governs the superparamagnetic relaxation through the relaxation time τ of the Arrhenius law:

$$\tau = \tau_0 \exp(K_{\text{eff}}V/k_BT). \tag{3}$$

The k exponent in Eqs. (1) and (2) is 1/2 for an assembly of aligned particles[20] and the coercive field follows the characteristic $T^{1/2}$-law. Pfeiffer has developed the case of an assembly of randomly oriented particles, obtaining that the coercive field also follows a T^k-law, with $k=0.77$ (See Ref. 33). H_c is plotted against $T^{1/2}$ and $T^{0.77}$ in the inset of Fig. 6(a) and in Fig. 6(b), respectively. Both approaches lead us to similar agreements with experimental results and they are followed only at the four lowest temperatures ($T<35$ K), since Eq. (1) is correct when most of the particles are blocked. The ZFC curve [Fig. 1(a)], the initial susceptibility χ_{in} (Fig. 7) and the ratio M_r/M_s [Fig. 8(a)] all suggest that this is accomplished at

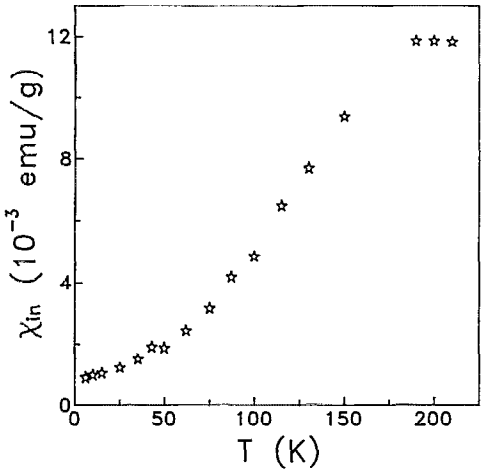

FIG. 7. Initial susceptibility χ_{in} (slope of the M vs H curve at low fields) for the Co-Ti sample.

low temperatures, far enough from the maximum of the ZFC curve ($T_M \approx 195$ K). The fitting of the experimental H_c values with Eq. (1) leads to $H_c(0)=5570$ Oe and $A=0.119$ K$^{-1/2}$ for the $T^{1/2}$-law, and to $H_c(0)=4690$ Oe and $A=0.043$ K$^{-0.77}$ for the $T^{0.77}$-law.

Assuming the characteristic values of τ_0 ($\tau_0 \approx 10^{-9}$–10^{-13} s) and of the measuring time of the experiment ($\tau_m \approx 50$–100 s for S.Q.U.I.D magnetometry) β may be estimated from $\beta=\ln(\tau_m/\tau_0)$ leading to $\beta=25$–34. β represents the ratio between the anisotropy energy and the thermal energy at which the relaxation time of a given particle is of the order of the measuring time of the experiment. This implies that, being the relationship between the two energies:

$$K_{\text{eff}}V \approx \beta k_B T, \tag{4}$$

the particles with volume V and anisotropy per unit volume K_{eff} are blocked at a temperature T. Taking the usual value $\beta=25$ (Ref. 20), although recent experiments show that β may be larger,[19] Eq. (2) and the experimental A values give an average energy $\langle K_{\text{eff}}V\rangle$ of about 2.4×10^{-13} erg (0.15 eV) and 2.1×10^{-13} erg (0.13 eV) for the $T^{1/2}$-law and $T^{0.77}$-law, respectively. $\langle K_{\text{eff}}V\rangle$ represents the mean height of the energy barrier distribution.

Concerning the isothermal magnetization curves, M may be written at low fields (below about 1000 Oe) as

$$M=\chi_{\text{in}}H, \tag{5}$$

where χ_{in} is the initial susceptibility, which is shown, as a function of temperature, in Fig. 7. The initial susceptibility increases more than one order of magnitude between 6 and 210 K and follows the ZFC magnetization perfectly [see Fig. 1(a)]. We should remark that the isothermal magnetization curves have always been recorded in the same way: We heat the sample up to room temperature and, then, we cool it in zero field down to the measuring temperature. We assume that both χ_{in} and M_{ZFC} variations come from the contribution of the superparamagnetic particles and this contribution increases with temperature up to T_M.

Above about 2000 Oe, the $M(H)$ curves were fitted to the law of approach saturation (LAS) for ferromagnetic and ferrimagnetic powders[21]

$$M=M_0(1-A/H-B/H^2)+\chi_d H, \tag{6}$$

where M_0 is the zero-field saturation magnetization and χ_d is the high-field differential susceptibility. χ_d is due to the contribution of noncollinear spins in the magnetic structure and it appears frequently in M-type doped ferrites as a consequence of the disruption of the collinear uniaxial magnetic structure when doping with diamagnetic cations. These cations induce the supression of some superexchange paths that facilitate the magnetic equilibrium, leading to new noncollinear magnetic structures.[22] Apart from this contribution, surface effects arising from noncollinear surface spins are also important in small particles. The A/H term is related to the existence of inhomogeneities in the microcrystals which reduce the mobility of the magnetization[23] and theoretically should vanish at high enough magnetic fields,[24] otherwise the magnetic energy necessary to saturate the sample would be infinite. This result has indeed been confirmed experimentally.[25] The B/H^2 term is related to the magnetic anisotropy and it may be written for a uniaxial hexagonal compound with $K_2 \ll K_1$[3,26]

$$\begin{aligned} B/H^2 &= 1/15(H_a/H)^2 C_B, \\ H_a &= H_k - H_{\text{sh}}, \end{aligned} \tag{7}$$

where H_k is the magnetocrystalline anisotropy field of a uniaxial system, with $H_k=2K_1/M_0^{\max}$, and K_1 is the first anisotropy constant.[3] H_{sh} represents the shape anisotropy field,[3] expressed as $H_{\text{sh}}=\Delta N M_0^{\max}$, ΔN being the difference between the demagnetizing factors along the easy and hard directions of a particle. As a first approximation, we will take $\Delta N=4\pi 0.54$ for the powder sample, corresponding to an aspect ratio (diameter-to-thickness ratio) $D/t \approx 4$, which is a typical average ratio for this kind of sample.[8,14] C_B is the volume fraction of ferrimagnetic (blocked) particles. Within the framework of the ideal Stoner–Wohlfarth model, we should expect that

$$M_r/M_s = 0.5 C_B, \tag{8}$$

where M_r is the remanent magnetization and 0.5 is the value of the M_r/M_s ratio at $T=0$ ($C_B=1$, all particles blocked). It is clear from Fig. 8(a) that $M_r/M_s<0.5$ as we approach $T\to 0$, which might be due to different facts, such as noncoherent rotational magnetization processes, interparticle interaction, magnetization reversal through tunneling, distribution of anisotropy fields, and particle size distribution. We may obtain an estimate of the fraction of blocked particles as a function of temperature from the expression

$$C_B(T)=(M_r/M_s)/(M_r/M_s)_{T\to 0}, \tag{9}$$

where $(M_r/M_s)_{T\to 0}$ is the value of the remanent-to-saturation ratio at $T\to 0$. As we cannot measure below 35 K since the sample is not saturated, we take $(M_r/M_s)_{T\to 0} \approx 0.3$ from the extrapolation of Fig. 8(a), as-

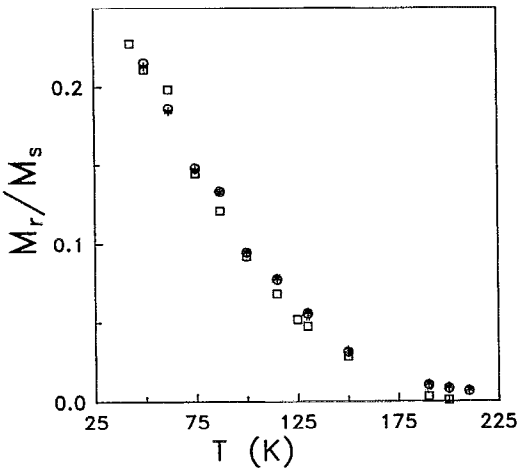

(a)

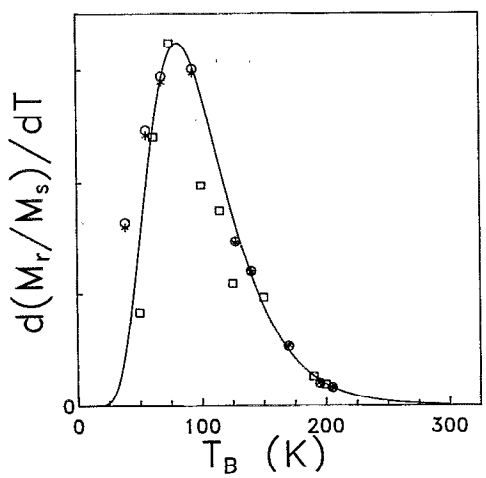

(b)

FIG. 8. (a) Remanent-to-saturation magnetization ratio as a function of temperature for the Co-Ti sample: (□) M_r/M_s, (○) $M(10\ \text{Oe})/M_s$, and (*) $M(10\ \text{Oe})/M_s(T=115\ \text{K})$. (b) derivative of the same data with respect to temperature, as a function of temperature. Solid line corresponds to the best fit of the data to a lognormal distribution.

suming that this ratio is saturated at $T\to 0$. Equation (6) can be applied only when the volume fraction of blocked particles is dominant with respect to that of superparamagnetic particles. At the mean blocking temperature $\langle T_B\rangle$ [$\langle T_B\rangle=81$ K, see below and Fig. 8(b)], $M_r/M_s\approx 0.14$, which indicates that about 50% of the total sample volume is ferrimagnetic (blocked). Then, we cannot fit the experimental $M(H)$ curves to the law of approach saturation expressed in Eq. (6) when $T>\langle T_B\rangle$.

The fitted values of χ_d (about 1.4×10^{-4} emu/g from 35 K up to $\langle T_B\rangle$) are larger than that obtained for the same Co-Ti $x=0.8$ compound prepared by the conventional ceramic method (about 0.4×10^{-4} emu/g at 4.2 K),[11] suggesting that χ_d increases as particle size decreases, as has been observed experimentally in the pure phase,[27] as a result of the enhancement of the finite-size effects.[28] The same is observed in the M_0 values (M_0 is about 18.8 emu/g from 35 K up to $\langle T_B\rangle$), which are much smaller than those of microscopic particles (about 90 emu/g at 4.2 K).[11]

From these results, we understand that there is a large dead magnetic layer at particle surface, which behaves as paramagnetic and contributes to the high-field differential susceptibility. Then, as experimental saturation magnetization (both M_0 and M_s) concern the whole particle (not only the inside core where magnetic structure is that of a bulk specimen, but also the dead magnetic layer), the volume of the magnetic unit must be related only to the inside core. This is the reason why we have used the experimental value of the zero-field saturation magnetization for microcrystalline particles $M_0^{\max}$ ($M_0^{\max}=90$ emu/g at 4.2 K, Ref. 11) in the definition of both the first anisotropy constant K_1 and the shape anisotropy H_{sh} ($K_1=1/2(H_k M_0^{\max})$, $H_{\text{sh}}=\Delta N M_0^{\max}$). In addition, we have introduced an effective anisotropy constant K_{eff} in Eqs. (2)–(4), since in the present case the shape anisotropy is not negligible. K_{eff} is related to the anisotropy field $H_a=H_k-H_{\text{sh}}$ through $K_{\text{eff}}=1/2(H_a M_0^{\max})$.

We notice that we have checked the purity of the sample by different ways in order to exclude the presence of spurious phases that lead to a reduction of the experimental saturation magnetization. The Curie temperature has been obtained with a vibrating sample magnetometer (VSM). The experimental value ($T_c\approx 633$ K) is very close to the value obtained for microcrystalline powders. The evolution of the magnetization with temperature up to T_c is regular and reversible, and no anomaly is observed, thus suggesting that other magnetic phases, if present, are below the detection limit of the apparatus. Moreover, the nucleation and growth of the ferrite phase have been followed carefully by chemical methods (thermogravimetry, kinetics), allowing to assert that the M-type phase is the major phase in the sample. Finally, although x-ray diffraction patterns have been also recorded, Bragg peaks are so broad that no conclusion concerning minor phases in the sample may be drawn from them.

The fitted magnetocrystalline anisotropy fields H_k are about 23 kOe between 35 K and $\langle T_B\rangle$. The anisotropy fields H_a are about 20 kOe in this temperature range. H_a and H_k are sensitive to the magnetic field interval where they are fitted. It is actually difficult to separate the A/H term from the B/H^2 term when fitting experimental $M(H)$ curves to Eq. (6). Only with magnetic fields well above 2–3 times the anisotropy field (which are not achievable with our experimental setup) may we be sure that the magnetization curves are purely of the $1/H^2$-type. We have fitted experimental curves to the $1/H^2$ term within magnetic field ranges always above 10 kOe, by fixing the $1/H$ contribution fitted below 10 kOe. We have detected relative enhancements of the values given above which are always below 25%. The first anisotropy constant K_1 and the effective anisotropy constant K_{eff} are about 5.5×10^6 erg/cm^3 and 4.7×10^6 erg/cm^3, respectively, between 35 K and $\langle T_B\rangle$, with a relative enhancement due to the fitting interval which is also below 25%.

All these results should be taken as approximate values for the following reasons: (i) the anisotropy fields derived from the law of approach saturation[29] are overestimated [in comparison with those obtained from other methods, such

as the singular point detection method (SPD)[30] and the transverse susceptibility method[30]], since we measure the larger values of the distribution of anisotropy fields $g(H_a)$, instead of the mean value. (ii) superparamagnetic particles contribute to the law of approach saturation through the Langevin function $L(x)=\coth(x)-1/x$, with $x=VM_sH/(k_BT)$. $L(x)$ is $1-1/x$ when x is large, and it is linear with x when x is small. As a result, the ratio VH/T determines if superparmagnetic particles contribute either to the $1/H$ term (and, therefore, this cannot be univocally attributed to crystal defects) or to the initial susceptibility χ_{in}. Also, at intermediate values of x, $L(x)$ may cause some uncertainty in the determination of the anisotropy field. We notice that x is of the order of 2.3 when $V=\langle V\rangle$, $T=\langle T_B\rangle$ (see below) and $H=1000$ Oe, if we use M^0_{max}. (iii) as the sample is polycrystalline, we will have some scattering in the demagnetizing factor ΔN. (iv) it is difficult to separate the A/H from the B/H^2 contribution, in the considered magnetic field range. The determination of the anisotropy field from independent methods is in progress now.

The fitted magnetocrystalline anisotropy fields H_k are larger than that reported for microcrystalline particles of the pure $BaFe_{12}O_{19}$ phase (about 17 kOe at 4.2 K),[3] and for the Co-Ti $x=0.8$ sample (about 13 kOe at 4.2 K, Ref. 11). Referring to the first anisotropy constant K_1, the fitted values are of the same order of magnitude as those reported for the pure phase (4.4×10^6 erg/cm^3 at 4.2 K and 3.2×10^6 erg/cm^3 at 300 K, Ref. 3) and are larger than those of the Co-Ti $x=0.8$ compound [3×10^6 erg/cm^3 at 4.2 K (Ref. 11) and 1×10^6 erg/cm^3 at 300 K (Ref. 31)].

All these results suggest that surface effects are of the greatest importance for nanocrystalline M-type barium ferrite particles and they seem to indicate that when reducing particle size, M_0 strongly decreases and H_k, K_1, and K_{eff} are enhanced with respect to the bulk values (K_1 and K_{eff} have been derived assuming that the inside core is responsible for the magnetic properties). Consequently, we suggest that the anisotropy comes from two different sources, one from the volume of the inside core and the other from the limit surface of this core. Therefore, the anisotropy constant K for nanocrystalline barium ferrite particles might be written as $K=K_b+(S/V)K_s$, where K_b is the anisotropy constant corresponding to the bulk (in erg/cm^3), K_s is the anisotropy constant corresponding to the surface of the inside core (in erg/cm^2) and S is the limit surface of the inside core. According to this expression, K increases when particle size decreases.

The ratio H_c/H_a is expected to be 0.48 in the classical Stoner–Wohlfarth model[32] (array of randomly oriented single domain noninteracting ferro/ferrimagnetically monodisperse particles). In our case, this should be accomplished at the limit $T\to0$, when all particles are blocked. However, $H_c(0)/H_a(0)$ is of the order of 0.2–0.3, much smaller than the expected value, as we have already detected in the remanence-to-saturation ratio. The same reasons that in that case might account for this reduction.

The ratio M_r/M_s is displayed in Fig. 8(a). From the derivative of M_r/M_s with respect to temperature we have extracted the distribution of blocking temperatures $F(T_B)$, corresponding to the distribution of particle volumes $f(V)$. We have fitted $F(T_B)$ to lognormal distribution [Fig. 8(b)]

$$F(T_B)=1/(\sqrt{2\pi}\sigma T_B)\exp[-1/(2\sigma^2)\ln^2(T_B/T_{B0})], \tag{10}$$

where $\ln(T_{B0})$ is the mean value of $\ln(T_B)$ and σ is an adimensional parameter associated with the dispersion around $\ln(T_{B0})$. The mean T_B value and its dispersion σ_T are written $\langle T_B\rangle=T_{B0}\exp(-\sigma^2)$ and $\sigma_T=T_{B0}\mathrm{sqr}[\exp(2\sigma^2)-\exp(\sigma^2)]$. Equation (10) and the experimental $d(M_r/M_s)/dT$ vs T curve lead to $\langle T_B\rangle=81$ K and $\sigma_T=40$ K. Then, the maximum of the M_{ZFC} curve T_M and $\langle T_B\rangle$ are related through $T_M=c\langle T_B\rangle$ with $c\approx2.4$, which represents about a 20% excess with respect to the $c=2$ value expected for a quasinormal distribution. We attribute this variation to the experimental error in the M_r/M_s data. Furthermore, Fig. 8(b) indicates that nearly all particles are superparamagnetic at room temperature, while all particles are blocked below about 20 K.

As the distribution of blocking temperatures $F(T_B)$ and the distribution of particle volumes $f(V)$ are related through Eq. (4), $\langle T_B\rangle$ leads us to a mean anisotropy energy $\langle K_1V\rangle\approx(2.8\pm1.4)\times10^{-13}$ erg, which is in good agreement with the mean values 2.4×10^{-13} erg and 2.1×10^{-13} erg that we have derived from the H_c vs $T^{1/2}$- and H_c vs $T^{0.77}$- laws [see Eqs. (1)–(4)]. Taking the mean value of the effective anisotropy constant K_{eff} of about 4.7×10^6 erg/cm^3 (we neglect the distribution of anisotropy fields), the mean volume of the magnetic unit $\langle V\rangle$ is $(6\mp3)\times10^4$ Å^3, smaller than the mean particle volume obtained from TEM ($\langle V\rangle\approx1.1\times10^5$ Å^3, Ref. 16), as expected when there is a large dead magnetic layer at particle surface. We notice that this particle volume, together with $D/t\approx4$, lead us to a specific surface area of about 271 m^2/g. Kubo *et al.* report[34] that the saturation magnetization of some barium ferrite samples ($x=0$, 0.5, 0.85, with some particle sizes for each substitution) significantly decreases when the surface specific area increases within 5 and 35 m^2/g. We believe that the extrapolation of this decrease till the specific surface area of the sample may explain the saturation magnetization that we find experimentally.

IV. SUMMARY AND CONCLUSIONS

We have studied the static magnetic properties of three different M-type doped barium ferrite compounds prepared by the glass crystallization method.

The ZFC and FC curves of all samples display the typical features of a small particle system. The ZFC processes present a broad peak at a temperature T_M, which depends on the particle size distribution. TEM shows that the larger the mean particle volume, the higher T_M. There is also a clear irreversibility between the ZFC and FC curves, which tends to disappear as we approach the superparamagnetic region.

A wide magnetic characterization of the Co-Ti compound has been recorded. Saturation magnetization fol-

lows a T^{α}-law above 120 K, with $\alpha \approx 2.7$. We suggest that relaxation effects may preclude the observation of spins waves at low temperature, while we detect the characteristic contribution of interacting spins waves at high temperature. However, we notice that small particles present α coefficients[18,19] which strongly depend on particle size. Coercive fields H_c follow a T^k-law below 35 K. Experimental values are in close agreement, within the experimental error, with both $k=1/2$ (aligned case)[20] and $k=0.77$ (random case),[33] where we obtain an estimate of the mean energy of anisotropy $\langle K_{\text{eff}} V \rangle$, leading to 2.4×10^{-13} and 2.1×10^{-13} erg, respectively. Above 35 K, the linearity is lost due to the contribution of superparamagnetic particles.

Isothermal magnetization curves have been fitted to the LAS expressed in Eq. (6) below the mean blocking temperature $\langle T_B \rangle$. The zero-field saturation magnetization M_0 is much smaller and the high-field differential susceptibility χ_d is much larger than the experimental values for microcrystalline particles. We ascribe this to finite-size effects.[27,28] We understand that there is a large dead magnetic layer at particle surface. Furthermore, the anisotropy constant K_1 and the anisotropy field H_k, which we associated with the inside core of the particle where the magnetic structure is that of a bulk specimen, are larger than those reported for microcrystalline particles. We suggest that the anisotropy of nanocrystalline barium ferrite particles comes from both the volume and the limit surface of the inside core.

The distribution of blocking temperatures has been attained from the derivative of remanent-to-saturation ratio with respect to temperature, which has been fitted to a lognormal distribution. We obtain that the mean blocking temperature $\langle T_B \rangle$ is (81 ± 40) K, leading to a mean energy of anisotropy $\langle K_{\text{eff}} V \rangle \approx (2.8\pm1.4)\times10^{-13}$ erg, in good agreement with mean values derived from the H_c vs T^k-laws. As the effective anisotropy constant K_{eff} is about 4.7×10^6 erg/cm^3, the mean volume of the magnetic unit is $(6\mp3)\times10^4$ Å^3, smaller, as expected, than the mean particle volume $\langle V \rangle \approx 1.1\times10^5$ Å^3 obtained from TEM.

We conclude from our results that the GCM is successful in obtaining very small Co-Ti particles with a narrow distribution of sizes in comparison with microcrystalline powders. At present, dynamic magnetic measurements are being recorded. We are measuring the time dependence of the FC magnetization, and our main goals are to obtain some information about the energy barrier distribution and its dependence on the magnetic field and information about the relaxation mechanism as $T \to 0$.

[1] M. P. Sharrock and L. Josephson, IEEE Trans. Magn. **22**, 723 (1986); T. Fujiwara, IEEE Trans. Magn. **23**, 3125 (1987); M. P. Sharrock, IEEE Trans. Magn. **25**, 4374 (1989).

[2] M. H. Kryder, J. Magn. Magn. Mater. **83**, 1 (1990); P. Gerard, E. Lacroix, G. Marest, M. Duphy, G. Rolland, and B. Blanchard, *ibid.* **83**, 13 (1990).

[3] H. Kojima, *Ferromagnetic Materials*, edited by E. P. Wohlfarth (North-Holland, Amsterdam, 1982), Vol. 3; J. Smith and H. P. Wijn, *Ferrites* (Philips Technical Library, Eindhoven, 1960).

[4] F. Licci and T. Besagni, IEEE Trans. Magn. **20**, 1639 (1984); M. Vallet, P. Rodríguez, X. Obradors, A. Isalgué, J. Rodríguez, and M. Pernet, J. Phys. Paris Colloq. **46**, C6-335 (1985).

[5] K. Haneda, C. Miyakawa, and H. Kojima, J. Am. Ceram. Soc. **57**, 354 (1974); W. Ross, *ibid.* **63**, 601 (1989).

[6] M. Kiyama, T. Takada, N. Nagai, and N. Horiishi, Adv. in Ceram. **15**, 51 (1985).

[7] B. T. Shirk and W. R. Buessem, J. Am. Ceram. Soc. **53**, 192 (1970); T. Ido, D. Eng, O. Kubo, Y. Hirotaka, and S. Kenjo, Toshiba Rev. **154**, 10 (1985); T. Fujiwara, IEEE Trans. Magn. **21**, 1480 (1985); P. Görnert, Prog. Cryst. Growth Charact. **20**, 263 (1990).

[8] P. Görnert, E. Sinn, and M. Rösler, Key Eng. Mater. **58**, 129 (1991); P. Görnert, E. Sinn, W. Schüppel, H. Pfeiffer, M. Rösler, Th. Schubert, M. Jurisch, and R. Sellger, IEEE Trans. Magn. **26**, 12 (1990); M. Rösler, P. Görnert, and E. Sinn, Z. Phys. **D19**, 279 (1991).

[9] O. Kubo, T. Ido, and H. Yokoyama, IEEE Trans. Magn. **18**, 1112 (1982); O. Kubo, T. Ido, H. Yokoyama, and Y. Koike, J. Appl. Phys. **57**, 4280 (1985).

[10] X. Batlle, J. Rodríguez, X. Obradors, M. Pernet, M. Vallet, and J. Fontcuberta, J. Phys. Paris Colloq. **49**, C8-939 (1988); X. Batlle, M. Pernet, X. Obradors, and M. Vallet, in *Advances in Ferrites*, edited by C. M. Srivastava and M. J. Patni (Oxford and IBH Publishing, New Delhi, 1989), p. 423.

[11] X. Batlle, X. Obradors, J. Rodríguez-Carvajal, M. Pernet, M. V. Cabañas, and M. Vallet, J. Appl. Phys. **70**, 1614 (1991).

[12] J. C. Slonczewski, Phys. Rev. **110**, 1341 (1958); D. J. De Bitetto, J. Appl. Phys. **35**, 3482 (1964); F. Bolzoni and L. Pareti, J. Magn. Magn. Mater. **42**, 44 (1984).

[13] M. Pernet, X. Obradors, M. Vallet, T. Hernandez, and P. Germi, IEEE Trans. Magn. **24**, 1998 (1988).

[14] P. Görnert, E. Sinn, H. Pfeiffer, W. Schüppel, and M. Rösler, J. Magn. Soc. Jpn. **15**, 669 (1991).

[15] Japan Technology Highlights, Vol. 2, No. 20, November 18, 1991.

[16] P. Görnert and E. Sinn (private communication).

[17] C. Kittel, in *Introduction to Solid State Theory* (Wiley, New York, 1971), 4th ed., p. 544; N. W. Ashcroft and N. M. Mermin, in *Solid State Physics* (Holt, Rinehart, and Winston, New York, 1976), p. 707.

[18] P. V. Hendriksen, S. Linderoth, and P. A. Lindgård, JMMM **104–107**, 1577 (1992).

[19] S. Linderoth, L. Balcells, A. Labarta, J. Tejada, P. V. Hendricksen, and S. A. Sethi, J. Magn. Magn. Mater. (to be published).

[20] C. P. Bean and J. D. Livingstong, J. Appl. Phys. **30**, 120S (1959).

[21] R. Grossinger, Phys. Status Solidi A **66**, 665 (1981); J. Magn. Magn. Mater. **28**, 137 (1982).

[22] R. A. Sadykov, O. P. Aleshko-Ozhevskii, and N. A. Arten'em, Sov. Phys. Solid State **23**, 1090 (1981); X. Obradors, A. Collomb, M. Pernet, and J. C. Joubert, J. Magn. Magn. Mater. **44**, 118 (1984); A. Collomb, X. Obradors, A. Isalgué, and D. Fruchart, J. Magn. Magn. Mater. **69**, 317 (1987).

[23] L. Neel, J. Phys. **9**, 148 (1948); J. Phys. Radium **9**, 184 (1948).

[24] L. Néel, J. Phys. **9**, 193 (1948).

[25] A. T. Aldred and P. H. Froehle, Int. J. Magn. **2**, 195 (1972).

[26] N. Akulov, Z. Phys. **69**, 822 (1931); R. Graus, Ann. Phys. **15**, 28 (1932).

[27] X. Batlle, X. Obradors, M. Medarde, J. Rodríguez-Carvajal, M. Pernet, and M. Vallet, J. Magn. Magn. Mater. **124**, 228 (1993).

[28] J. M. D. Coey, Phys. Rev. Lett. **27**, 1140 (1971); S. Kuriso, T. Ido, and H. Yokoyama, IEEE Trans. Magn. **23**, 3137 (1987); K. Haneda and A. H. Morrish, IEEE Trans. Magn. **25**, 2597 (1989).

[29] R. Ardiaca, R. Ramos, A. Isalgué, J. Rodríguez, X. Obradors, M. Peret, and M. Vallet, IEEE Trans. Magn. **23**, 22 (1987).

[30] G. Asti and S. Rinaldi, J. Appl. Phys. **45**, 3600 (1974); L. Pareti and G. Turilli, J. Appl. Phys. **61**, 5098 (1987).

[31] F. Chou, X. Feng, J. Li, and Y. Lin, J. Appl. Phys. **61**, 3381 (1987).

[32] E. C. Stoner and E. P. Wohlfarth, Philos. Trans. R. Soc. London Ser. A **240**, 599 (1948).

[33] H. Pfeiffer and W. Schüppel, Phys. Status Solidi A **119**, 259 (1990); H. Pfeiffer, *ibid.* **120**, 233 (1990).

[34] T. Ido, O. Kubo, H. Yokoama, and S. Kenjo, Toshiba Review **154**, 10 (1985).